Hindawi Publishing Corporation
International Journal of Photoenergy
Volume 2011, Article ID 314702, 6 pages
doi:10.1155/2011/314702

Research Article

Photoemission Spectroscopy Characterization of Attempts to Deposit MoO_2 Thin Film

Irfan,[1] Franky So,[2] and Yongli Gao[1,3]

[1] *Department of Physics and Astronomy, University of Rochester, Rochester, NY 14627, USA*
[2] *Department of Materials Science and Engineering, University of Florida, Gainesville, FL 32611-6400, USA*
[3] *Institute for Super Microstructure and Ultrafast Process (ISMUP), Central South University, Changsha, Hunan 410083, China*

Correspondence should be addressed to Irfan, irfan4phy@gmail.com

Received 15 July 2011; Revised 13 September 2011; Accepted 20 September 2011

Academic Editor: Wayne A. Anderson

Copyright © 2011 Irfan et al. This is an open access article distributed under the Creative Commons Attribution License, which permits unrestricted use, distribution, and reproduction in any medium, provided the original work is properly cited.

Attempts to deposit molybdenum dioxide (MoO_2) thin films have been described. Electronic structure of films, deposited by thermal evaporation of MoO_2 powder, had been investigated with ultraviolet photoemission and X-ray photoemission spectroscopy (UPS and XPS). The thermally evaporated films were found to be similar to the thermally evaporated MoO_3 films at the early deposition stage. XPS analysis of MoO_2 powder reveals presence of +5 and +6 oxidation states in Mo 3d core level along with +4 state. The residue of MoO_2 powder indicates substantial reduction in higher oxidation states while keeping +4 oxidation state almost intact. Interface formation between chloroaluminum phthalocyanine (AlPc-Cl) and the thermally evaporated film was also investigated.

1. Introduction

Applications of organic semiconductors (OSCs) are increasingly attracting interest of both scientific and industrial communities because of its low synthesis cost and tunable material properties. Potential applications, including organic photovoltaic cells (OPVs) [1–3], organic light emitting diodes (OLEDs) [4–6], and organic thin film transistors (OTFTs) [7, 8], have been successfully demonstrated. Despite the impetus from these early successful applications, tremendous scope of performance enhancement is expected with proper understanding of each interface in the organic device. Therefore, detailed investigations are desired for each interface with the characterization of electronic structure and interface energy level alignments.

A great deal of efforts have been made in order to improve the charge transport and collection at the electrodes. Introduction of a high work function (WF) transition metal oxide insertion layer between conducting indium tin oxide (ITO) and organic semiconductors was an attempt first made by Tokito et al. [9]. While improvement of device performance is well established with the oxide insertion layer [10–13], consensus on the mechanism of this improvement is yet to be achieved. Kroger et al. [14, 15] have reported a possible mechanism for hole injection improvement, originating from electron extraction from the highest occupied molecular orbital (HOMO) of organic semiconductor to the ITO anode through conduction band of MoO_3. In our reports [13–16], we have established the efficiency enhancement by a reduced hole injection barrier and a drift field from hole accumulation in the organic material at the ITO/hole injection layer interface. We have also underlined the importance of the high work function (WF) of MoO_3 for the performance enhancement of devices [16–19]. Some other groups have emphasized on gap-state-assisted transport [20]. The role of defect states on performance has also been raised by many research groups [21–23]. Greiner et al. [21] and Vasilopoulou et al. [22] have recently reported that the reduced molybdenum trioxide film (MoO_x and $x \sim 2.7$) outperforms the stoichiometric trioxide film, due to the presence of defect states in the former. These reports invoke interest in the investigation of MoO_2 film as an interlayer.

In the present, work we discuss our investigation of MoO_2 deposition attempts and the interface formation with

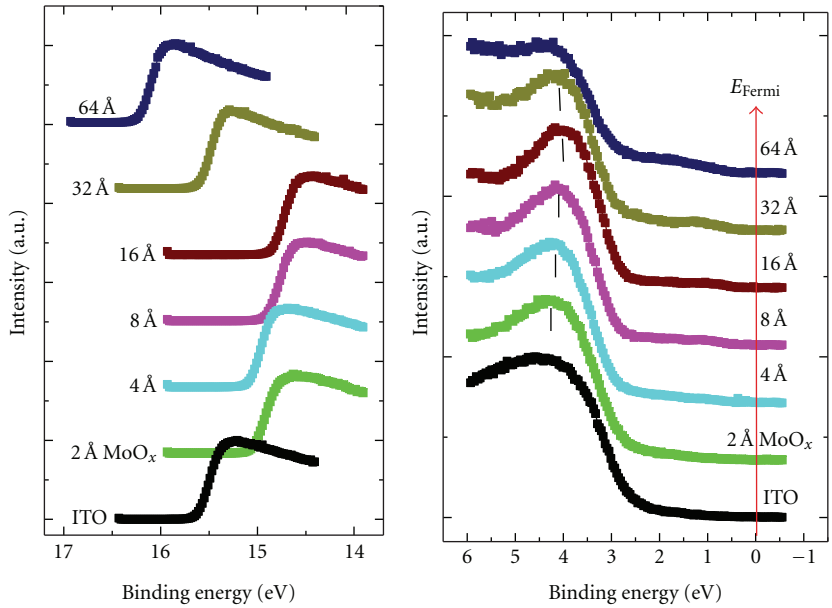

Figure 1: UPS data for ITO, 2 Å, 4 Å, 8 Å, 16 Å, 32 Å, and 64 Å MoO_2 for (a) the cut-off region and (b) the valence region.

chloroaluminum phthalocyanine (AlPc-Cl) using ultraviolet photoemission spectroscopy (UPS) and X-ray photoemission spectroscopy (XPS). We investigated the electronic properties of films deposited by thermally evaporated MoO_2 powder. At the early stage of MoO_2 evaporation, the electronic structure of the deposited film resembles to that of thermally evaporated MoO_3 thin films [16–19, 24]. We probed molybdenum 3d core level spectra for MoO_2 powder and residue powder from MoO_2 evaporation boat to compare the difference. We observed strong reduction in +6 oxidation state, while +4 oxidation state was almost intact. We also studied the interface formation of the deposited film (by thermal evaporation of MoO_2 powder) with AlPc-Cl, and results are discussed.

2. Experimental Details

UPS measurements were performed using a VG ESCA Lab UHV system equipped with a He discharge lamp. The UHV system consists of three interconnecting chambers, a spectrometer chamber, an in situ oxygen plasma (OP) treatment chamber, and an evaporation chamber. The base pressure of the spectrometer chamber is typically 8×10^{-11} torr. The base pressure of the evaporation chamber is typically 1×10^{-6} torr. The UPS spectra were recorded by using unfiltered He I (21.22 eV) excitation, as the excitation source with the sample biased at −5.00 V to observe the low-energy secondary cutoff. The UV light spot size on the sample is about 1 mm in diameter. The typical instrumental resolution for UPS measurements ranges from 0.03 to 0.1 eV with the photon energy dispersion of less than 20 meV. XPS spectra were measured with a Surface Science Laboratories' SSX-100 system equipped with a monochromatic Al anode X-ray gun (Kα 1486.6 eV). The base pressure of the system is 9×10^{-11} torr. The spot size of the X-ray was selected to be 1000 micron in diameter. The resolution of this system is 0.5 eV. One of the substrate was a borosilicate glass from Corning, coated with 250 nm thick conducting ITO, with resistivity 15 Ω per square. The ITO substrate was treated in situ in oxygen ambience of 600 milli-torr at bias voltage of −500 V for 30 sec in the VG system's evaporation chamber. Other substrates were cut from gold-coated Si wafer. All the substrates were roughly about 8 mm × 8 mm in size. All the substrates were ultrasonically cleaned before being loaded in to the UHV chambers. All the measurements were performed at room temperature.

3. Results and Discussion

3.1. Thin Film Deposited on Indium Tin Oxide (ITO) by Evaporation of MoO_2 Powder. Thermally deposited thin films from MoO_2 powder on indium tin oxide (ITO) were investigated with ultraviolet photoemission spectroscopy (UPS). The current required for the early evaporation was 1.5 times higher than the current required for the thermal evaporation of MoO_3 powder. The thermal evaporation of MoO_2 powder was performed in the evaporation chamber of the VG ESCA system, as described in the experimental details. The evaporation became harder with increasing deposition, and beyond 64 Å, the current required was more than twice of usual current for the thermal evaporation of MoO_3 powder. At such a high current, the pressure in the preparation chamber was $\sim 1 \times 10^{-3}$ torr from usual 1×10^{-6} torr and eventually the evaporation boat broke/melted down due to excessive heat.

In Figure 1, the UPS data are presented for the cut-off region (a) and the valence band region (b), with increasing thickness of the thermally evaporated films. All the spectra

have been normalized to the same height for visual clarity. The data presented in the cut-off region provides a quick visualization of surface work function (WF) changes. The cut-off binding energy (BE) position of oxygen-plasma-(OP-) treated ITO surface is measured to be 15.49 eV from which the WF of 5.73 eV can be measured by subtracting photon energy (21.22 eV). The WF first increased with the evaporated film thickness up to 16 Å and then started to decrease. The WF at 2 Å, 4 Å, 8 Å, and 16 Å thicknesses were measured to be 6.28 eV, 6.24 eV. 6.42 eV, and 6.48 eV, respectively. The WF after the 16 Å thickness started to decrease and was found 5.72 eV and 5.10 eV for 32 Å and 64 Å film thickness, respectively. The initial (upto 16 Å thickness) WF enhancement is associated with +6 and +5 oxidation state of molybdenum oxide rather than +4. The reported work function value of MoO_3 thin film is 6.7 ± 0.2 eV [13–19]. The highest occupied molecular orbital (HOMO) region as presented in Figure 1(b) provides a quick visualization of changes in the occupied levels (valence band region for inorganic materials) lying within few eV of binding energy (BE) with respect to the Fermi level of the system. In Figure 1(b), we notice a clear change in the valence region from ITO to 2 Å film thickness. With the 2 Å thickness, we observed the characteristic molybdenum trioxide peak with the peak position at 4.25 eV [15]. Increasing the MoO_2 evaporation thickness results in the peak position at 4.17 eV, 4.09, and 4.00 eV for 4 Å, 8 Å, and 16 Å thicknesses, respectively. The shift of ~0.2 eV in the valence band peak towards the lower BE is similar to the shift of WF from 2 Å to 16 Å thickness. These shifts indicate a minor electron trap at the interface of MoO_x/ITO. At 8 Å thickness we observed a gap state around ~1 eV and an another gap state start to appear around ~2 eV at 64 Å thickness. The valence band spectra of initial 2 Å and 4 Å thicknesses is exactly similar to the thermally evaporated MoO_3 films [15]. The presence of oxychloride formation at the AlPc-Cl/MoO_x interface could not be ascertained but cannot be completely ruled out [6].

3.2. XPS of MoO_2 and Residue MoO_2 Powder. In order to further confirm the preferential evaporation of molybdenum trioxide and molybdenum suboxide at early stage rather than molybdenum dioxide, we performed X-ray photoemission spectroscopic (XPS) measurements on MoO_2 powder and residue MoO_2 powder from inside of an evaporation boat after ~20% of the filled MoO_2 powder from the boat was evaporated. Both MoO_2 and the residue powder were mixed with methanol to make it like a paste. The pastes were dropped on gold substrates and were automatically dried after methanol was quickly evaporated. Both the samples were then transferred in the SSX-100 system for the XPS measurements.

In Figure 2(a), Mo 3d core levels are presented for MoO_2 powder and the residue. We observed different oxidation state of molybdenum in MoO_2 powder itself. The presence of higher oxidation states was puzzling. The origin of the formation of higher oxidation state may be due to absorption of oxygen from air or by decomposition of unstable MoO_2 molecules in to the metallic and higher oxidation states. A quick comparison between MoO_2 and the residue vividly illustrates the preferential reduction of higher oxidation states of molybdenum in the residue. In Figure 2(b), peak fitting Mo 3d spectrum of MoO_2 powder is performed. The peak fitting was done with fixed separation of 3.2 eV for $3d_{5/2}$ and $3d_{3/2}$ spin orbit coupling splitted peaks, fixed area ratio of 3 : 2, and the same full width at half the maximum height (FWHM) for both the peaks. The positions of $3d_{5/2}$ peaks of +4, +5, and +6 oxidation state of molybdenum were measured to be 228.83 eV, 230.36 eV, and 232.00 eV, respectively. The observed peak positions agree well with earlier reports [21, 25, 26]. The percent intensity of +4, +5, and +6 oxidation states of molybdenum were measured to be 22%, 19%, and 59%, respectively. In Figure 2(c), peak fitting of Mo 3d spectrum of residue MoO_2 powder is presented. The positions of $3d_{5/2}$ peaks of +4, +5, and +6 states were found to be 228.77 eV, 230.37 eV, and 232.01 eV, respectively. The intensity of +4, +5, and +6 oxidation states was measured to be 37%, 33%, and 30%, respectively. While the intensity reduction of +4 and +5 oxidation states was small in the residue, the +6 oxidation state was reduced to one fourth. The above finding is consistent with our observation in the first section that the evaporation of MoO_2 powder at early stage results mostly in MoO_3 deposition.

3.3. Interface Formation of MoO_2 with Chloroaluminum Phthalocyanine (AlPc-Cl). After being convinced that the early stage evaporation of MoO_2 results in the deposition of MoO_3 and after few nanometers a little mixture of oxide of molybdenum with lower oxidation states, we performed interface formation of MoO_2 evaporated film with AlPc-Cl. Interface formation is crucial in order to understand possible device performance and possibly comment on the controversy of performance enhancement by molybdenum trioxide versus suboxide interlayer between an organic semiconductor and the electrode. The current required for the early evaporation of MoO_2 powder was 1.5 times higher than the current required for the thermal evaporation of MoO_3 powder. In the present study, the thermal evaporation of MoO_2 powder was performed inside the VG ESCA system, as described in the experimental section. The evaporation became harder with increasing deposition, and, beyond 30 Å thickness, the current, required was more than twice of usual current for the thermal evaporation of MoO_3 powder. At such a high current the pressure in the preparation chamber was $\sim 1 \times 10^{-5}$ torr from usual 8×10^{-11} torr, and we stopped further evaporation of MoO_2 powder. AlPc-Cl was deposited in the preparation chamber, on top of the 30 Å MoO_2 powder evaporated film.

In Figure 3, the UPS data are plotted for the cut-off region (a) and the highest occupied molecular orbital (HOMO) region (b) with increasing thickness of MoO_2 evaporated film and then AlPc-Cl films. All the spectra have been normalized to the same height for visual clarity. In Figure 3(a), the WF of gold substrate was measured to be 5.0 eV. The surface WF first increased with the deposition of 5 Å and 10 Å film and was measured to be 6.51 eV and 6.68 eV, respectively. With further deposition of MoO_2 WF was measured to be 6.25 eV and 5.49 eV, respectively. The WF reduction may be originating due to contribution of oxides

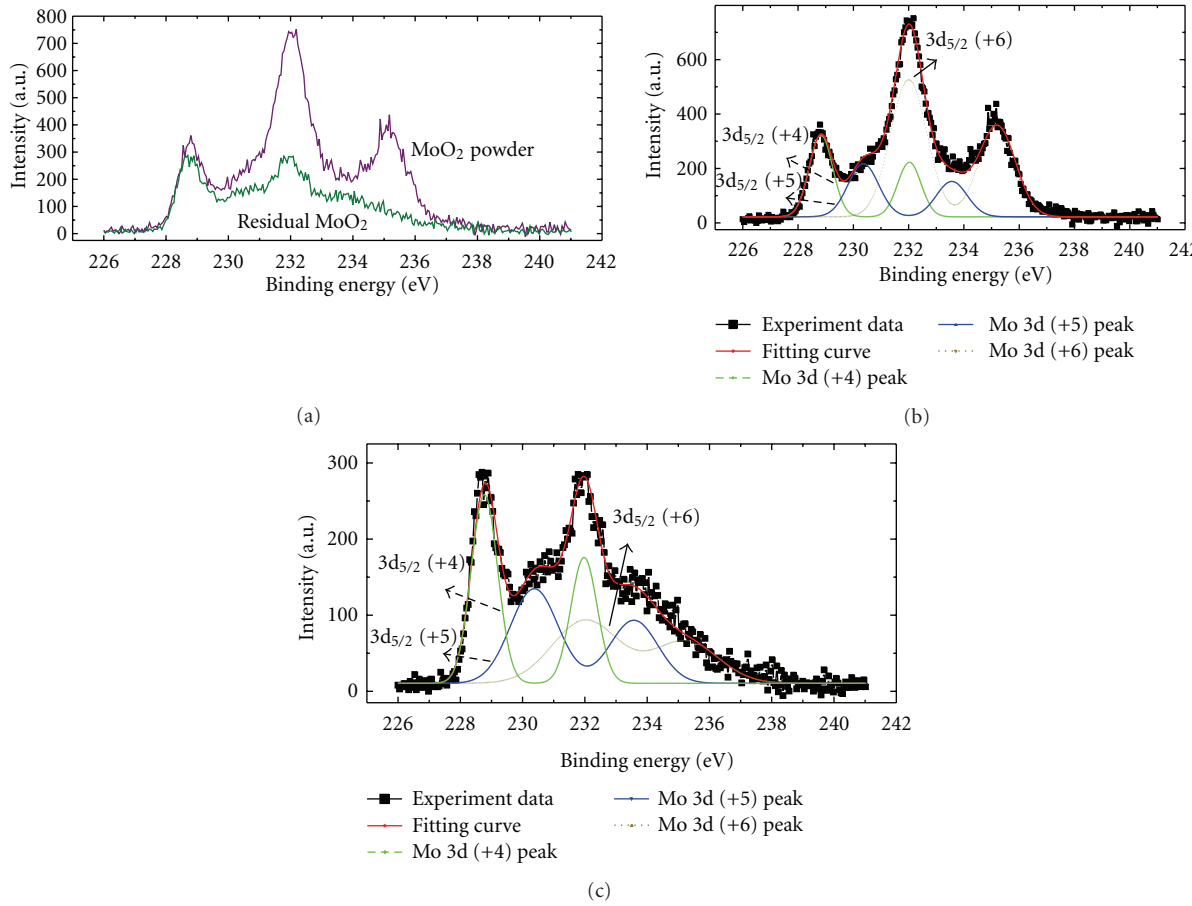

Figure 2: XPS data of molybdenum 3d core level, (a) MoO_2, powder, and residual MoO_2 powder, (b) peak fitting of Mo 3d spectrum for MoO_2 powder, and (c) peak fitting of Mo 3d spectrum for residual MoO_2 powder.

of molybdenum with lower oxidation state, or exposure of deposited MoO_3 film [17–19] to unavoidable high pressure inside the chamber due to excessive heat in the MoO_2 evaporation boat, or a combination of both. After the deposition of the 30 Å film, we deposited AlPc-Cl layer by layer on top. With deposition of AlPc-Cl, the WF continuously decreased before reaching a saturation value of 4.82 eV at 32 Å thickness. In Figure 3(b), we observed the Fermi edge from the substrate. The early evaporation of MoO_2 again results in the valence region spectra similar to that of MoO_3 [16, 17]. With the deposition of AlPc-Cl on 30 Å MoO_2 film, the features of AlPc-Cl [16, 17] started to appear. The HOMO features of AlPc-Cl became prominent between 4 Å to 8 Å thickness, and the HOMO onsets were measured to be 0.45 eV and 0.47 eV, respectively. With further increase in the AlPc-Cl thickness, there was no significant change.

The energy level alignment at the AlPc-Cl/MoO_3 interface [16] is dramatically different than at the AlPc-Cl/MoO_2 evaporated film interface. The early HOMO onset value of 0.45 eV observed in the present case is more than 1.5 times of 0.28 eV observed with MoO_3. Energy levels are more or less flat with the increasing thickness of AlPc-Cl in the present case, while there was strong band-bending-like region in the case of AlPc-Cl/MoO_3 interface. In the absence of band-bending-like region, the expected hole extraction should not be efficient. Thus, with MoO_2 evaporated film interlayer, at the early stage, the larger value of hole injection barrier and later the absence of drift electric field would make it less efficient. We attribute this change to the low work function of deposited film either due to the contribution of oxides of molybdenum with lower oxidation states than +6 or exposure of early deposited MoO_3 film.

4. Conclusion

In conclusion, we presented investigations on MoO_2 evaporated film insertion layer and interface formation with an organic semiconductor. We observed that the early stage MoO_2 evaporation results in MoO_3 deposition marked with high surface work function. After few nm of evaporation, we observed the deposited film to have some contribution of lower oxidation state of molybdenum, marked with low work function and a prominent defect state at the binding energy around ~2 eV. Our X-ray photoemission study reveals the dramatic reduction in the +6 oxidation state of molybdenum in the residue MoO_2 powder. The interface formation of AlPc-Cl/MoO_2 evaporated film brings out the higher hole injection barrier and no band bending in AlPc-Cl, which

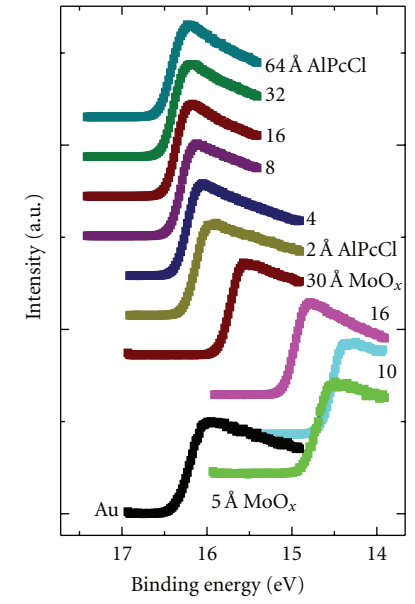

(a)

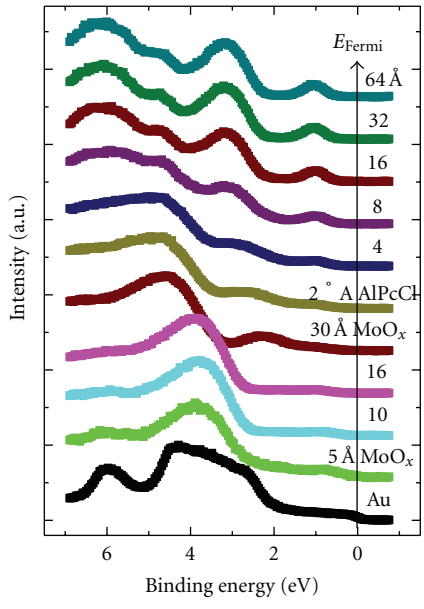

(b)

Figure 3: UPS data for Au, 5 Å MoO_2, 10 Å, 16 Å, 30 Å MoO_2, 2 Å AlPc-Cl, 4 Å, 8 Å, 16 Å, 32 Å, and 64 Å AlPc-Cl. (a) The cut-off region and (b) the HOMO region.

would hamper the device performance. Therefore, reduced MoO_3 oxide may be performing nicely the extreme reduction to MoO_2 which would have deleterious effects on the device performance.

Acknowledgment

The authors would like to acknowledge the support of the National Science Foundation Grant no. DMR-1006098.

References

[1] C. W. Tang, "Two-layer organic photovoltaic cell," *Applied Physics Letters*, vol. 48, no. 2, pp. 183–185, 1986.

[2] G. Yu, J. Gao, J. C. Hummelen, F. Wudl, and A. J. Heeger, "Polymer photovoltaic cells: enhanced efficiencies via a network of internal donor-acceptor heterojunctions," *Science*, vol. 270, no. 5243, pp. 1789–1791, 1995.

[3] G. Li, V. Shrotriya, J. Huang et al., "High-efficiency solution processable polymer photovoltaic cells by self-organization of polymer blends," *Nature Materials*, vol. 4, no. 11, pp. 864–868, 2005.

[4] C. W. Tang and S. A. Vanslyke, "Organic electroluminescent diodes," *Applied Physics Letters*, vol. 51, no. 12, pp. 913–915, 1987.

[5] R. H. Friend, R. W. Gymer, A. B. Holmes et al., "Electroluminescence in conjugated polymers," *Nature*, vol. 397, no. 6715, pp. 121–128, 1999.

[6] M. G. Helander, Z. B. Wang, J. Qiu et al., "Chlorinated indium tin oxide electrodes with high work function for organic device compatibility," *Science*, vol. 332, no. 6032, pp. 944–947, 2011.

[7] Z. Bao, A. J. Lovinger, and A. Dodabalapur, "Organic field-effect transistors with high mobility based on copper phthalocyanine," *Applied Physics Letters*, vol. 69, no. 20, pp. 3066–3068, 1996.

[8] G. Horowitz, "Organic field-effect transistors," *Advanced Materials*, vol. 10, no. 5, pp. 365–377, 1998.

[9] S. Tokito, K. Noda, and Y. Taga, "Metal oxides as a hole-injecting layer for an organic electroluminescent device," *Journal of Physics D: Applied Physics*, vol. 29, no. 11, pp. 2750–2753, 1996.

[10] F. X. Wang, F. X. Qiao, T. Xiong, and D. G. Ma, "The role of molybdenum oxide as anode interfacial modification in the improvement of efficiency and stability in organic light-emitting diodes," *Organic Electronics*, vol. 9, no. 6, pp. 985–993, 2008.

[11] V. Shrotriya, G. Li, Y. Yao, C. W. Chu, and Y. Yang, "Transition metal oxides as the buffer layer for polymer photovoltaic cells," *Applied Physics Letters*, vol. 88, no. 7, 2006.

[12] M. D. Irwin, D. B. Buchholz, A. W. Hains, R. P. H. Chang, and T. J. Marks, "p-Type semiconducting nickel oxide as an efficiency-enhancing anode interfacial layer in polymer bulk-heterojunction solar cells," *Proceedings of the National Academy of Sciences of the United States of America*, vol. 105, no. 8, pp. 2783–2787, 2008.

[13] D. Y. Kim, J. Subbiah, So Franky, H. Ding, Irfan, and Y. Gao, "The effect of molybdenum oxide interlayer on organic photovoltaic cells," *Applied Physics Letters*, vol. 95, no. 9, Article ID 093304, 2009.

[14] M. Kroger, S. Hamwi, J. Meyer, T. Riedle, W. Kowalsky, and A. Kahn, "Role of deep lying electronic states of MoO_3 in the enhancement of hole-injection in organic thin films," *Applied Physics Letters*, vol. 95, Article ID 123301, 3 pages, 2009.

[15] M. Kröger, S. Hamwi, J. Meyer, T. Riedl, W. Kowalsky, and A. Kahn, "P-type doping of organic wide band gap materials by transition metal oxides: a case-study on Molybdenum trioxide," *Organic Electronics*, vol. 10, no. 5, pp. 932–938, 2009.

[16] Irfan, H. Ding, Y. Gao, D. Y. Kim, J. Subbiah, and F. So, "Energy level evolution of molybdenum trioxide interlayer between indium tin oxide and organic semiconductor," *Applied Physics Letters*, vol. 96, no. 7, Article ID 073304, 2010.

[17] Irfan, H. Ding, Y. Gao et al., "Energy level evolution of air and oxygen exposed molybdenum trioxide films," *Applied Physics Letters*, vol. 96, no. 24, Article ID 243307, 2010.

[18] M. Zhang, Irfan, H. Ding, Y. Gao, and C. W. Tang, "Organic Schottky barrier photovoltaic cells based on MoO_x / C_{60}," *Applied Physics Letters*, vol. 96, no. 18, Article ID 183301, 2010.
[19] Irfan, M. Zhang, H. Ding, C. W. Tang, and Y. Gao, "Strong interface p-doping and band bending in C_{60}," *Organic Electronics*, vol. 12, no. 9, pp. 1588–1593, 2011.
[20] Y. Yi, P. E. Jeon, H. Lee et al., "The interface state assisted charge transport at the MoO_3/metal interface," *Journal of Chemical Physics*, vol. 130, no. 9, Article ID 094704, 2009.
[21] M. T. Greiner, M. G. Helander, Z. B. Wang, W. M. Tang, J. Qiu, and Z. H. Lu, "A metallic molybdenum suboxide buffer layer for organic electronic devices," *Applied Physics Letters*, vol. 96, no. 21, Article ID 213302, 2010.
[22] M. Vasilopoulou, L. C. Palilis, D. G. Georgiadou et al., "Reduced molybdenum oxide as an efficient electron injection layer in polymer light emitting diodes," *Applied Physics Letters*, vol. 98, no. 1, 2011.
[23] P.-S. Wang, I.-W. Wu, W.-H. Tseng, M.-H. Chen, and C.-I. Wu, "Enhancement of current injection in organic light emitting diodes with sputter treated molybdenum oxides as hole injection layers," *Applied Physics Letters*, vol. 98, no. 17, article 173302, 2011.
[24] R. T. Sobieraj, K. Hermann, M. Witko, A. Blume, G. Mestl, and R. Schlögl, "Properties of oxygen sites at the $MoO_3(010)$ surface: density functional theory cluster studies and photoemission experiments," *Surface Science*, vol. 489, no. 1–3, pp. 107–125, 2001.
[25] F. Werfel and E. Minni, "Photoemission study of the electronic structure of Mo and Mo oxides," *Journal of Physics C: Solid State Physics*, vol. 16, no. 31, pp. 6091–6100, 1983.
[26] C. D. Wagner, W. M. Riggs, L. E. Davis, J. F. Moulder, and G. E. Muilenberg, *Handbook of X-Ray Photoelectron Spectroscopy*, Perkin-Elmer Corporation, 1979.

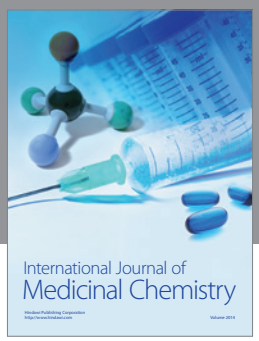

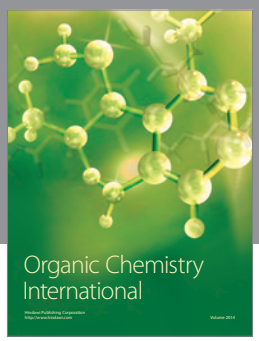

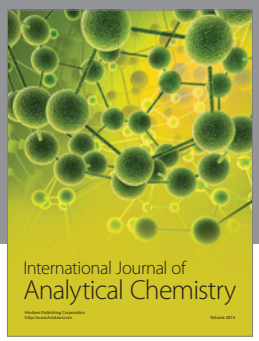

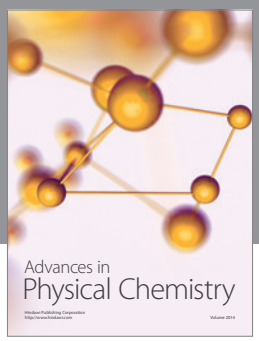

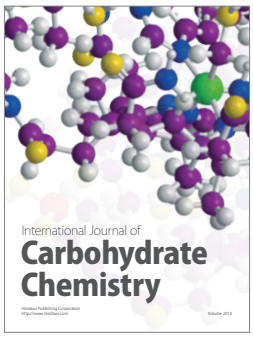

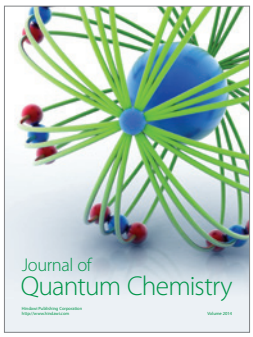

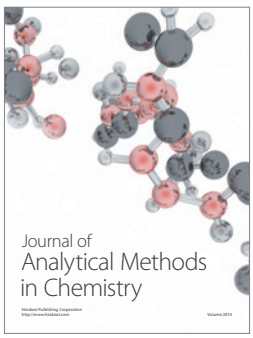

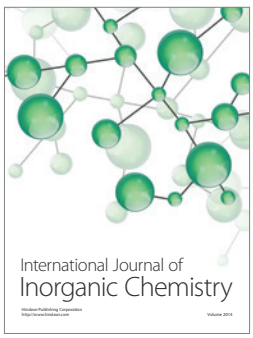

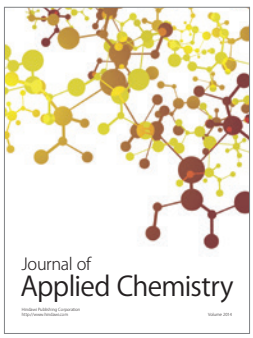

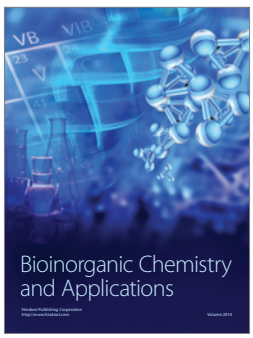

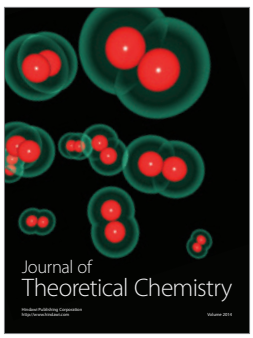

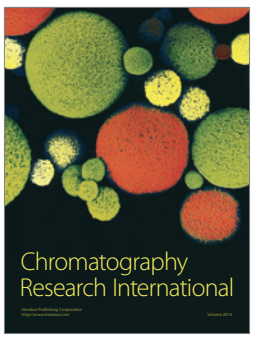

Hindawi

Submit your manuscripts at
http://www.hindawi.com